Response of Pile Points on Rock to Transient Loading

La Réponse des Pointes de Pieux sur Roche à une Charge Transitoire

H. BREDENBERG Civ.Eng., Royal Institute of Technology, Stockholm, Sweden
B.B. BROMS Professor, Royal Institute of Technology, Stockholm, Sweden

SYNOPSIS The dynamic response of pile points on hard rock to transient loads has been investigated experimentally. A theoretical relationship between the initial and the reflected stress waves and the dynamic point resistance is used to calculate the force-penetration relationship for the pile point. Computed and measured values have been compared. The stress-pulse was produced by a steel hammer striking a model pile. Due to the very short rise times of the stress wave, it was not possible to use standard accelerometers, inductive gauges or similar equipment. Resisistive gauges were used instead. The displacements were calculated by integrating the difference between the initial and the reflected stress waves. The experimental technique and the numerical algoritm used in this investigation are described. A bilinear force-displacement function is suggested so that initial low resistance of the rock can be taken into account.

INTRODUCTION

The dynamic response of point bearing piles driven to hard rock is of interest with respect to

- driveability
- integrity
- pile design and
- hammer selection

The main difference between the dynamic loading during driving and the static loading during the life of the structure is the duration of the applied load. During the driving the loading time may be as short as 0.1 millisecond, while the duration of the static load after the driving often is 10 to 100 years or more. The ratio of the duration of the loads can be as large as 10^{13}.

The static force-displacement relationship can be measured relatively easily and very accurately. The dynamic behaviour is much more difficult to determine. The best results, as far as piles are concerned, have been obtained with a comparatively simple semi-empirical two parameter model consisting of a linear spring and a dashpot (Goble et al, 1975). For hard rock when the rise time of the stress pulse can be as short as a few microseconds and the duration as short as a millisecond or less (see Fig. 1) it is difficult to measure the force and the penetration of the rock point as discussed in this paper.

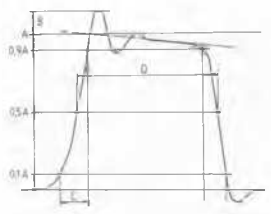

A = Amplitude
B = Overshot
C = Risetime
D = Duration

Fig. 1 Pulse Characteristics

THEORETICAL BACKGROUND

A steel pile is often long compared with the length of the stress wave generated during the driving. One-dimensional stress wave theory is therefore used for the theoretical analysis and calculations (Fischer et al, 1960).

The forces acting at the pile point are shown in Fig. 2.

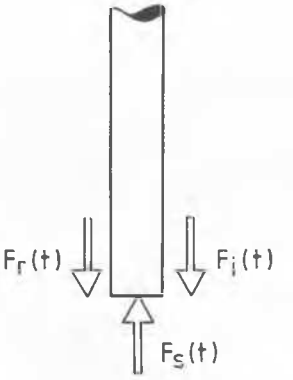

Fig. 2 Forces at a Pile Point

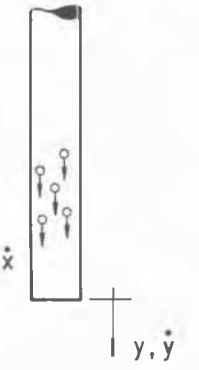

Fig. 3 Generalized Coordinates

At equilibrium of the pile point in Fig. 2

$$F_s(t) = F_i(t) + F_r(t) \qquad (1)$$

where $F_s(t)$ = point resistance

$F_i(t)$ = force of the initial stress wave

$F_r(t)$ = force of the reflected stress wave

The forces in Eq. (1) are all functions of time.

The relationship between the force (F) and the particle velocity ($\dot{x}$) for a cross section can be calculated from the wellknown expression

$$F = Z\dot{x} \qquad (2)$$

where Z = (AE/c) pile impedance

A = cross-sectional area of the pile

E = Young's modulus

$c = \sqrt{E/\rho g}$ longitudinal wave velocity

ρ = density

$\dot{x}$ = (dx/dt) particle velocity

From Eqs (1) and (2)

$$F_s(t) = Z\dot{x}(t) + Z\left[\dot{x}(t) - \dot{y}(t)\right] \qquad (3)$$

The point velocity $\dot{y}$ can then be calculated from

$$\dot{y}(t) = \frac{1}{Z}\left[2\,F_i(t) - F_s(t)\right] \qquad (4)$$

The displacement of the pile point is obtained by integrating Eq. (4):

$$y(t) = \frac{1}{Z}\int\left[2\,F_i(t) - F_s(t)\right]dt \qquad (5)$$

If Eqs. (1) and (2) are combined

$$y(t) = \frac{1}{Z}\int\left[F_i(t) - F_r(t)\right]dt \qquad (6)$$

This equation can be rewritten as

$$y(T) = \frac{\Delta t}{Z}\sum_{j=1}^{j=n}\left(2\,F_{i,j} - F_{r,j}\right) \qquad (7)$$

where $T = n\,\Delta t$

Δt = time increment

n = number of time increments

j = 1, 2, ..., n

The integration of this equation is illustrated in Fig. 4.

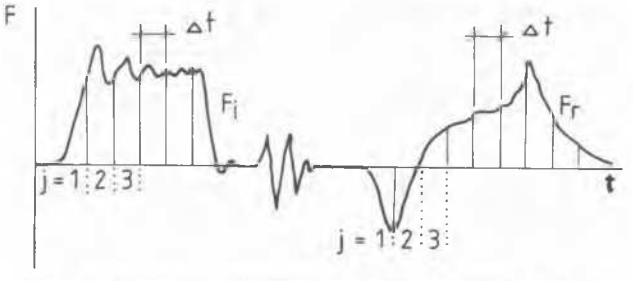

Fig. 4 Numerical Integration of Point Displacement

When the pile and the hammer have the same impedance, the initial wave will theoretically be rectangular. If the point support corresponds to a linear spring, the force-displacement relationships shown in Fig. 5 are obtained (Bredenberg and Broms, 1979) by integrating Eq. (4) with $F_i(t) = F_o$ for $0<t<t_o$, and $F_i(t) = 0$ at $t>t_o$.

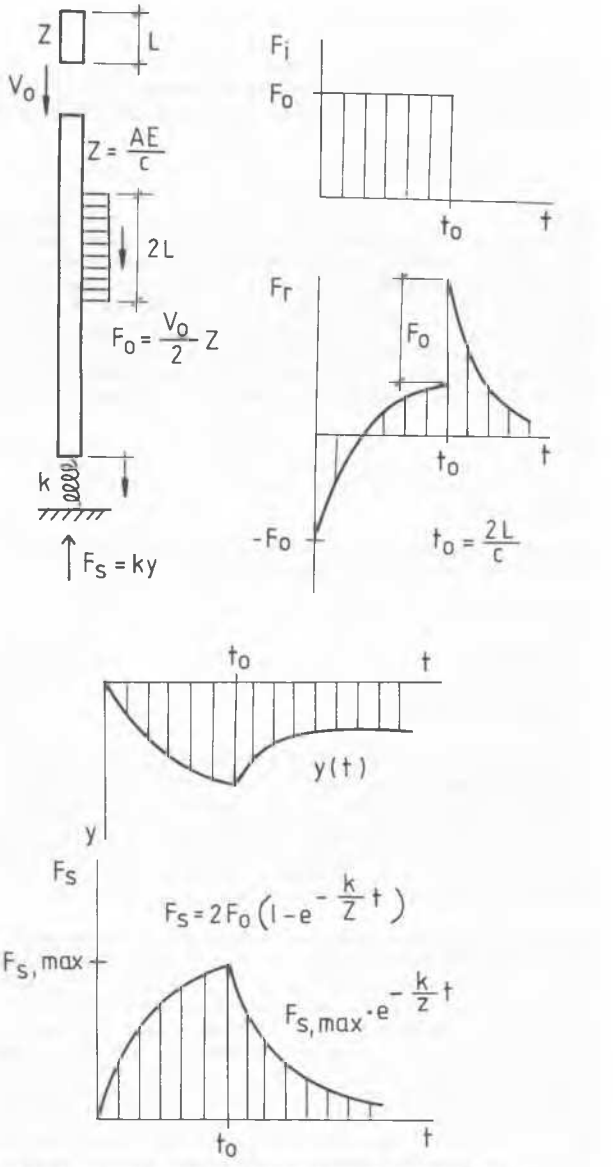

Fig. 5 Forces for a Linear Spring Point Model

The spring model in Fig. 5 is a simplification. In some cases, a spring combined with a friction coupling to simulate the elasto-plastic behaviour and a dash-pot will give a better indication of the effect of the velocity on the point resistance. However, for steel core piles driven to hard rock, the simplier linear model will be accurate enough and illustrate many important principles, e.g. the reflected tension wave and the exponential increase of the point resistance.

TEST EQUIPMENT

The test equipment which was used in this investigation is shown schematically in Fig. 6. A 500 mm long steel hammer with the same diameter (20 mm) as the 6 m long model pile was used. The pile rested on a granite block. The free falling hammer was guided by a transparent plastic tube. The height of fall was 1.0 m. Resistance strain gauges were placed 3.0 m (compensated for bending) and 5 cm above the pile point.

The signals from the gauges passed through a balancing circuit (Wheatstone bridge) and an amplifiers with 40 Hz limit frequency to a digital two-channel Nicolet 1090 memory oscilloscope. The initial and the reflected waves were recorded. The strain gauges at the centre of the bar were used. The signals from an analog output on the oscilloscope were divided into 512 equal time intervals with an HP-3582 spectrum analyzer and transfered to a LSI-11 minicomputer across an 8-bit IEEE-488 parallel data bus.

The results of the calculations were presented on a CRT and a X-Y plotter. With more modern digital oscilloscopes, the division into equidistant time values for subsequent processing in a computer can be made directly. The results are stored on a floppy disk.

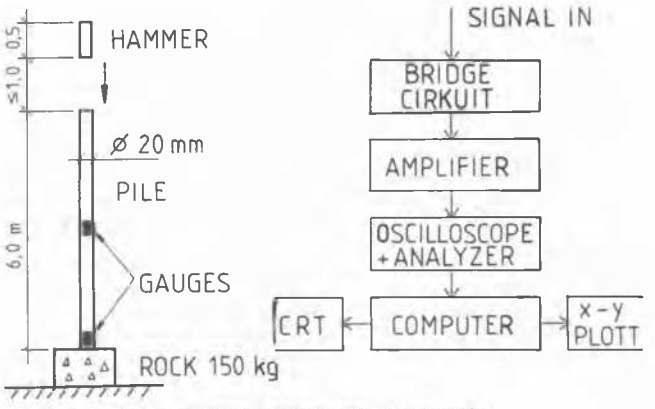

Fig. 6 Test Equipment, Schematic.

The rise time of the front of the stress wave is increased when the signals pass through the different measuring instruments. By applying a rectangular wave with a function generator at the measuring points, the rise time distorsion could be determined. It was about 3 µs and did not affect the calculations.

There is also a gradual decrease of the slope of the wave front and of the amplitude as the stress wave travels down through the bar due to dispersion. The dispersion increased the rise time of the reflected wave by about 5 µs compared with the initial wave. This increase was neglected in the calculations.

The force at the pile point was also measured. The agreement between measured and calculated values (Eq. 1) was good. The results were therefore considered to be reliable for transient loads mainly because of recent improvements of the electrical measuring devices. It is possible to improve the measurement system further with fast A/D converters and other sophisticated micro-electronic components.

The pile point was supported on a granite block. The Young's modulus determined on 15 mm diameter rock samples was 40 to 50 GPa. The unconfined compression strength measured using 20 mm diameter samples with a height of 40 mm varied between 200 and 250 MPa. The ultimate bearing capacity of a 20 mm diameter point made of special steel was about 450 kN, which corresponds to an average point pressure of 1400 MPa, or about six times the unconfined compressive strength of the rock.

TEST RESULTS

The initial as well as the theoretical stress wave assuming a linear spring point support for a hammer dropped from a height of 0.5 m are shown in Fig. 7. It can be seen that the agreement between calculated and measured values is fairly good. The differences are due to the simplified assumptions inherent in the one-dimensional stress wave propagation theory and the simplified spring model. The spring konstant (k) for the point was assumed to be 400 MN/m.

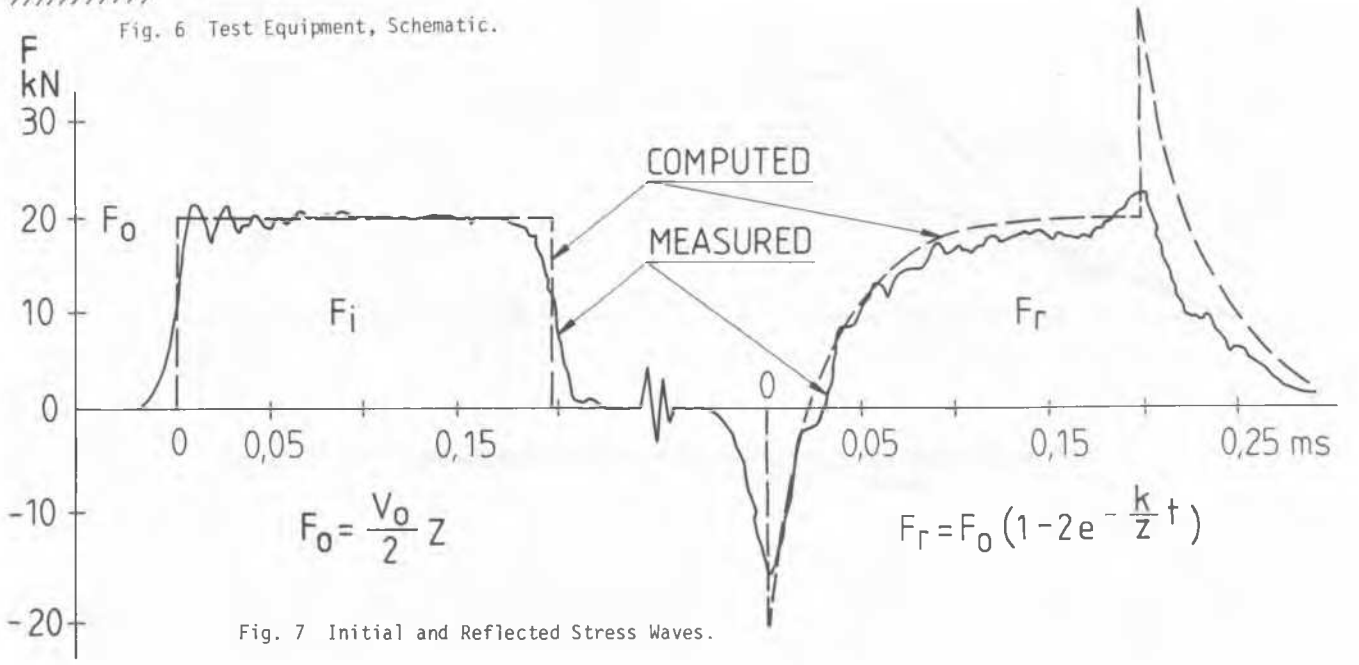

Fig. 7 Initial and Reflected Stress Waves.

As can be seen from the figure, the intensity of the reflected tension wave was somewhat smaller than calculated partly because the initial wave front was not infinitely steep. The maximum tension can be reduced by decreasing the rise time. This can be achieved in practice with a cushion at the top of the pile.

Fig. 8 shows the measured dynamic force - penetration curves of the pile point at the drop heights 0.25, 0.50, 0.75 and 1.00 m. The displacement was calculated from Eq. (7). The force at the point of the pile was calculated from Eq. (1). It was also measured with strain gauges (Fig. 6). There was a definite difference between the experimental results and the calculated values using a linear elastic spring model. The point resistance increased slowly until the movement of the point was about 0.10-0.15 mm. Thereafter the resistance increased much faster until the point force reached a maximum. At unloading the relationship was roughly linear.

The spring constant for the steep parts of the curves was about 400 MN/m which corresponds to a Young's modulus for the rock of about 20 GPa, using the relationship

$$k \approx Ed \qquad (8)$$

where d is the diameter of the pile point.

The relationship between the maximum intensity ($F_{i\ max}$) of the initial stress wave and the maximum point force ($F_{S\ max}$) in Fig. 8 is shown in Table 1.

TABLE 1

Maximum Intensity of the Initial Stress Wave and the Maximum Point Forces.

Drop height (m)	$F_{i,max}$ (kN)	$F_{s,max}$ (kN)	$F_{s,max}/F_{i,max}$
0.25	14.1	27.1	1.92
0.50	20.0	39.0	1.95
0.75	24.6	47.1	1.91
1.00	28.3	54.1	1.91

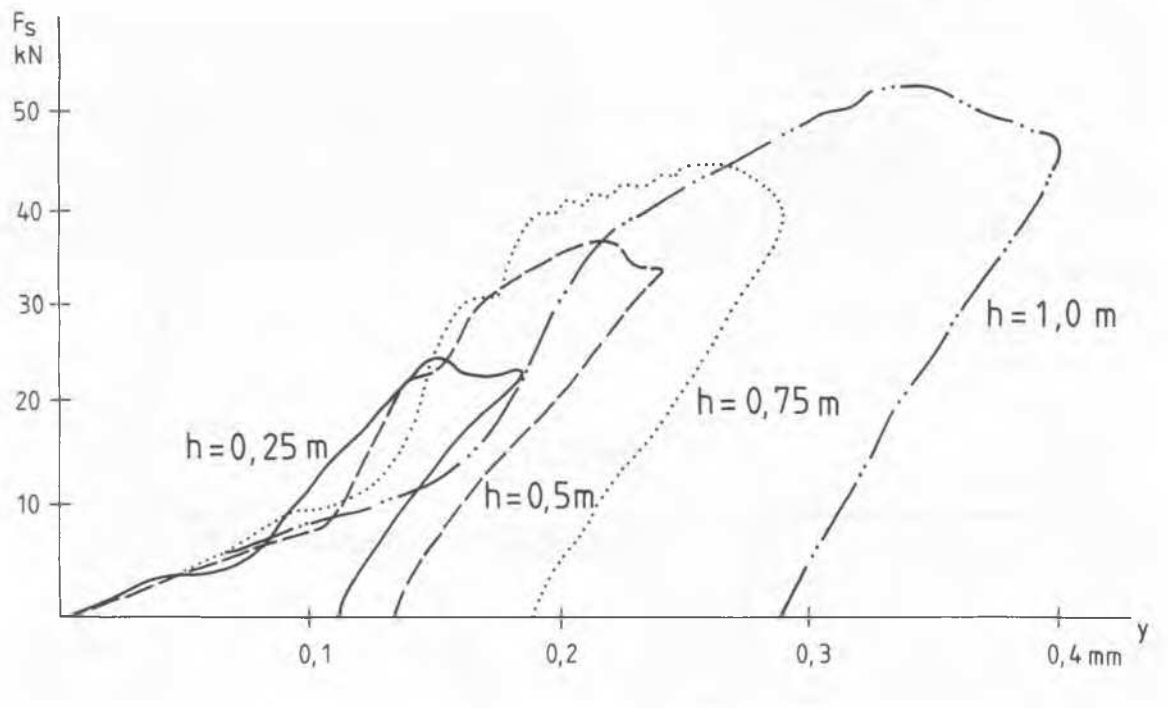

Fig. 8 Measured Force-Displacement Relationship (20 mm diameter pile point)

The area below the curves in Fig. 8 should be equal to the work by the pile point and the energy delivered by the hammer, the potential energy of the hammer with respect to the pile head before it was released. Numerical calculation of the expresson

$$W_s = \int_0^{y_{max}} F_s(y)\, dy \qquad (9)$$

where y_{max} = maximum displacement of pile point

W_s = work of pile point

{n Fig. 8 shows that about 5% to 10% of the energy of the hammer is lost mainly during the impact.

CONCLUSIONS

The length of the initial, less sloping part of the force-displacement relationship varied between the different test series. When the surface under the point had been thoroughly cleaned the spread could be reduced to about 10 to 20% of the values shown in Fig. 8. The actual dynamic point-force relationship for a single blow depends to a large extent on the contact between the pile point and the rock.

The bilinear elasto-plastic point model in Fig. 9a is frequently used. No permanent penetration occurs before a limiting displacement (the so-called quake value) has been reached. The results in Fig. 8 indicate that there is always a permanent penetration regardless of the magnitude of the point force. The actual maximum point force was only about 55 kN compared with a static ultimate bearing capacity of about 450 kN. Therefore the point force - point displacement relationship in Fig. 8 represents only a part of the real relationship.

The initial "soft" response of the pile tip is often overlooked at static load tests. At dynamic loading this low initial resistance has a large effect, especially on stress waves with a steep front. It is suggested that the force-displacement relationship shown in Fig 9b should be used instead.

The dynamic ultimate bearing capacity is somewhat larger than the corresponding static capacity, as shown by e.g. Hustrulid (1968). In our case, the introduction of a damping dash-pot to take this effect into account dit not improve the agreement between measured and calculated values.

The Young's modulus determined from the dynamic tests was smaller than that from the static load tests. One reason could be the decrease of the ultimate strength and of the stiffness when subjected to repeditive loading. In a previous investigation, it was noted that the ultimate load after 30 load cycles was only 80% of that when the rock first was loaded. The reduction after 1 000 load cycles was 50%. These tests were performed using a 20 mm diameter point on a granite surface (Rehnman and Broms, 1972). Similar results have been obtained for concrete.

It was very difficult to evaluate the peak point force accurately when only the permanent set was measured. It was much more reliable to measure directly the initial and reflected forces. In the field special equipment is available to do this today (Goble et al, 1975).

Stresses above the yield point caused plastic deformations of the steel point. The magnitude of these deformations depends on the duration of the plastification. Since the yield strength of the steel is about 200 to 400 MPa, it is often difficult to reach the ultimate load of hard rock without causing plastic deformation if high strength steel is not used.

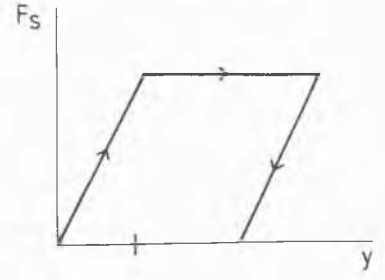

Fig. 9a Bilinear Point Model

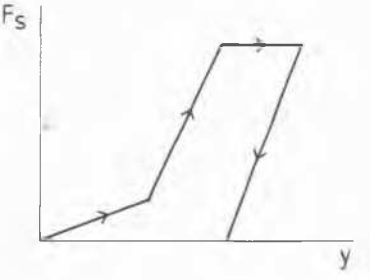

Fig. 9b Proposed Model

REFERENCES

Bredenberg, H. and Broms, B.B. (1979). Bearing capacity of steel core piles. Proc. ASCE 1979 Fall Convention, Atlanta, USA.

Fischer, H.C. (1960). On longitudinal impact IV, New graphodynamical pulse method for computing pile driving process. Applied Scientific Research, Vol. AIX, The Hague, The Netherlands.

Goble, G.G., Garland Likins Jr. and Rausche, F. (1975). Bearing capacity of piles from dynamic measurements. Final Report, Dept. of Civil Engineering, Case Western Reserve University, Cleveland, Ohio, USA.

Hustrulid, W.A. (1969). Theoretical and experimental study of percussive drilling of rock. Ph.D. thesis, University of Minnesota, USA.

Rehman, S.E. and Broms, B.B. (1972). Bearing capacity of end bearing piles. Swedish Geotechnical Institute, Reprints and Preliminary Reports, No. 44.